Romanian Reports in Physics, Vol. 68, No. 1, P. 138–150, 2016

COUPLING CONSTANT IN SHAPE FUNCTION MODEL

R. SALEH-MOGHADDAM, M. E. ZOMORRODIAN

[1]Department of Physics, Faculty of Sciences, Ferdowsi University of Mashhad, 91775-1436, Mashhad, Iran

Email: R_{-}saleh88@yahoo.com, zomorrod@um.ac.ir

Received May 29, 2014

Abstract. The shape function model is used to calculate the coupling constant in perturbation theory and also the non-perturbative free parameter concerned with the QCD theory. This analysis is based on employing the event shape observables $\langle B_T\rangle, \langle B_W\rangle, \langle 1-T\rangle$ and $\langle\rho\rangle$. By fitting the Monte Carlo data as well as the AMY data with the shape function distribution, we find combining the results of all variables. We have obtained the mean value of the strong coupling constant $\alpha_s(M_{Z^0}) = 0.115960.00778$ and the nonperturbative parameters $\lambda_1 = 1.07790.02276 GeV$. Our results are consistent with the values obtained from other experiments at different energies and QCD predictions. We explain all these features in this article.

Key words: Perturbative calculations, Monte Carlo methods, Hadron production.

1. INTRODUCTION

The interactions between the constituents of matter are successfully described by the weak, electromagnetic, strong and gravitational forces. The weak and the strong interactions occur at small atomic to subatomic distances, the electromagnetic interaction is observed at subatomic to macroscopic distances while effects of Gravitation only play a role at macroscopic distances. The strong interaction, the main focus of this article, is responsible for the existence of all composite elementary particles (hadrons) by providing the binding force between the constituents and also for most of the short lived hadron decays. Furthermore, the binding of protons and neutrons in nuclei may be explained in analogy to chemical binding of molecules based on the strong interaction of the proton and neutron constituents. A dynamic theory of strong interactions at the constituent level, Quantum Chromo Dynamics (QCD), is constructed as a renormalized field theory in close analogy to Quantum Electro Dynamics (QED), the quantum field theory of the electromagnetic interaction. QCD is referred to as a non-abelian gauge theory while QED is an example of an abelian gauge theory. For massless quarks the strong coupling constant α_S is the only free parameter of the theory [1].

There are different methods for computing the strong coupling constant. This parameter belongs to perturbative theory. Furthermore there is a free parameter in non-perturbative part. The dispersive model [2] and the shape function model are two ways among the common methods for calculation of these parameters. The above models are based on non-perturbative theory. These parameters are calculated by using the dispersive model [2]. We extend this analysis by using the shape function model. Then we compare our obtained values from the shape function model with the values in the dispersive model and QCD predictions.

The outline of the paper is as the following. In section 2, we consider the event shape variables used in this analysis. Section 3 describes the power corrections as well as the perturbative QCD predictions, and also introduces the shape function model which describes the hadronization process. We present our results in section 4, using the simulated as well as the AMY data. Section 5 is devoted to our conclusion.

2. EVENT SHAPE OBSERVABLES

Event shape variables measure geometrical properties of hadronic final states at high energy particle collisions. They have been studied at e^+e^- collider experiments. Apart from distributions of these observables, we can also study the mean values as well as higher orders for the moments of event shape variables. The most common observables (y) are: thrust, the heavy jet mass, the total and wide jet broadening. We use the following event shape observables:

a) Thrust (T): This observable is defined by the expression [3]:

$$T = max(\frac{\sum_i |\overrightarrow{p_i} \cdot \overrightarrow{n}|}{\sum_i |\overrightarrow{p_i}|}) \tag{1}$$

where p_i is the momentum of reconstructed particle *i* in an event. The thrust axis $\overrightarrow{n}_T$ is the direction $\overrightarrow{n}$ for which the maximum occurs. We will use the form $1-T$ here since its distribution is in this form more similar to those of the other observables.

b) Jet Broadening (B): The definitions of the jet broadening observables employ a plane through the origin perpendicular to the thrust axis $\overrightarrow{n_T}$ to divide the event into two hemispheres S_1 and S_2. The Total and the Wide Jet Broadening B_T and B_W are defined as [4]:

$$B_k = (\frac{\sum_{i \in S_k} |\overrightarrow{p_i} \times \overrightarrow{n_T}|}{2\sum_i |\overrightarrow{p_i}|}) \tag{2}$$

for each of the two hemispheres $(S_k, k = 1, 2)$, defined above. The wide jet broadening is given by:

$$B_W = max(B_1, B_2) \tag{3}$$

The total jet broadening is defined by:

$$B_T = B_1 + B_2 \tag{4}$$

c) Heavy Jet Mass (M_H): The plane orthogonal to the thrust axis divides the space into two hemispheres S_1 and S_2. An invariant mass is calculated from the particles in each of the two hemisphere defined by the thrust axis. The hemisphere masses are defined by:

$$M_i^2 = (\sum_{j \in S_i} p_j)^2, (i = 1,2) \tag{5}$$

where p_j denotes the four momentum of particle *j*. The heavy hemisphere mass M_H is then defined by:

$$M_H^2 = max(M_1^2, M_2^2) \tag{6}$$

The above variable is scaled by the visible energy which is after correction for detector resolution, acceptance, and for initial state radiation, equals to:

$$\rho = \frac{M_H^2}{Q^2} \tag{7}$$

where Q is the centre of mass energy.

For these observables complete, $O(\alpha_s^2) + NLO$ QCD predictions as well as power correction calculations for their differential distributions are available.

3. THE SHAPE FUNCTION MODEL

The value of α_s can be assessed by the energy dependence of mean values of event shape distributions. The mean values of the observables considered in this analysis are calculated up to $O(\alpha_s^2)$ [2]. Korchemsky and Tafat [5] describe properties of the event shape variables $1-T$ and M_H^2 not included in NLO perturbation theory by a so called shape function, which does not depend on the variable nor the centre of mass energy. This is more general than the dispersive model, considering both as a shift of the perturbative prediction and as a compression of the distribution peak. The prediction is deduced from studying the two jet region in the distribution of the event shape variable *y*. The prediction for the differential distribution is:

$$\frac{1}{\sigma}\frac{d\sigma}{dy} = \int_0^{Q_y} d\varepsilon \, f_y(\varepsilon) \frac{d\sigma_{NLO}}{dy} \, (y - \frac{\varepsilon}{Q}) \tag{8}$$

with a non-perturbative function $f_y(\varepsilon)$, dependent on one scale parameter ε. This function is derived from the shape function $f(\varepsilon_L, \varepsilon_R)$ [5], which depends on two scale parameters $\varepsilon_L, \varepsilon_R$ for the two hemispheres of the event. By the compression of the distribution the validity of the prediction is extended compared to the dispersive model to $y \backsim \frac{\Lambda_{QCD}}{Q}$.

It has been observed many years ago that for some event shape variables like thrust and heavy jet mass perturbative QCD predictions deviate from the data by corrections suppressed by powers of the large energy scale $\frac{1}{Q^p}$ with the exponent p depending on the variable and $p = 1$ for T and ρ variables [6]. For the mean value $\langle y \rangle$ the leading power correction is parameterized by a non-perturbative scale λ_p of dimension p, while hadronization corrections to the differential distribution are described by a function $f_{had}(Q,y)$ depending on both the shape variable and the centre-of-mass energy

$$\frac{1}{\sigma_{tot}}\frac{d\sigma}{dy} = \frac{d\sigma_{PT}}{dy} + f_{had}(Q,y) \tag{9}$$

y denoting a general event shape variable ($y = 1-T, \rho, C, ...$) and the subscript PT referring to perturbative contribution, $\langle y \rangle_{PT} = \int y \frac{d\sigma_{PT}}{dy} dy$. Obviously, the hadronization corrections to the differential distributions have a richer structure than those to the mean values.

$$\langle y \rangle = \langle y^{pert} \rangle + \langle y^{pow} \rangle = \frac{1}{\sigma_{tot}} \int y \frac{dy}{d\sigma} d\sigma \tag{10}$$

This ansatz provides an additive term to the perturbative $O(\alpha_s^2)$ QCD prediction [7].

For an observable event, the perturbative prediction is:

$$\langle y^{pert} \rangle = \overline{A}_F (\frac{\alpha_s(\mu)}{2\pi}) + (\overline{B}_F + \overline{A}_F\, \beta_0\, log(\frac{\mu^2}{Q^2})\,(\frac{\alpha_s(\mu)}{2\pi})^2 \tag{11}$$

where $\overline{A}_F = A_F, \overline{B}_F = B_F - (\frac{3}{2}) C_F A_F, \beta_0 = \frac{(33-2N)}{12\pi}$ and μ being the renormalization scale. The coefficient A_F and B_F were determined from the $O(\alpha_s^2)$ perturbative calculations. Also Q is centre of mass energy in this equation. QCD color factors are: $C_A = 3$ and $C_F = \frac{N^2-1}{2N} = \frac{4}{3}$ for $N = 3$ (color number) [8].

For instance, non-perturbative scales λ_p parameterzing power corrections to $\langle y^{pow} \rangle$ is defined by the moment $\int y f_{had}(Q,y) dy$ [6].

$$\langle y \rangle = \langle y \rangle_{PT} + \frac{\lambda_p}{Q^P} \tag{12}$$

The terms with the derivatives of $\frac{1}{\sigma}\frac{d\sigma_{PT}}{dy}$ generate the series of power corrections accompanied by the set of non-perturbative μ-dependent dimensionful parameters $\langle y^n \rangle$ that can be expressed in terms of the scales λ_p introduced as [7].

The *nth* moment of an event shape observable y is defined by:

$$\langle y^n \rangle = \int_0^{y_{\max}} y^n \frac{1}{\sigma_{had}} \frac{d\sigma}{dy} dy \tag{13}$$

y_{max} is the kinematically allowed upper limit of the observable. This leads to the non-perturbative predictions.

$$\langle y^n \rangle = \int_0^\infty d\varepsilon\, y^n f(y;\mu),\ \langle y \rangle = \lambda_1,\ \langle y \rangle^2 - \langle y^2 \rangle = \lambda_2,\ \ldots \tag{14}$$

The shape function can be parameterized by its first moment,

$$\lambda_1 = \int d\varepsilon_R \int d\varepsilon_L (\varepsilon_R + \varepsilon_L) f(\varepsilon_L, \varepsilon_R) \equiv \langle \varepsilon_R + \varepsilon_L \rangle. \tag{15}$$

Its "second moment",

$$\lambda_2 = \langle (\varepsilon_R + \varepsilon_L)^2 \rangle. \tag{16}$$

In the following we calculate the power correction in dispersive model [2]. Such calculations correspond to the shape function model mentioned above, but we have made below, minor modifications for higher moments, that is we replace the $a_y.P$ by $\frac{\lambda_1}{Q}$ in the shape function for the first order power correction, and similarly for higher corrections.

$$\langle y^1 \rangle = \langle y^1 \rangle_{NLO} + a_y.P \tag{17}$$

$$\langle y^2 \rangle = \langle y^2 \rangle_{NLO} + 2\langle y^1 \rangle_{NLO}(a_y.P) + (a_y.P)^2 \tag{18}$$

$$\langle y^3 \rangle = \langle y^3 \rangle_{NLO} + 3\langle y^2 \rangle_{NLO}(a_y.P) + \langle y^1 \rangle_{NLO}(a_y.P)^2 + (a_y.P)^3 \tag{19}$$

$$\langle y^4 \rangle = \langle y^4 \rangle_{NLO} + 4\langle y^3 \rangle_{NLO}(a_y.P) + 6\langle y^2 \rangle_{NLO}(a_y.P)^2$$

$$+4\langle y^1 \rangle_{NLO}(a_y.P)^3 + (a_y.P)^4 \tag{20}$$

Predictions for event shape variables in shape function model for non-perturbative parameters can be derived, λ_1 and λ_2 can also be obtained from fit to the data [7].

From prediction (8) for the distribution of the variables $1-T$ and ρ, we can calculate the mean values with respect to non-perturbative distributions [6].

$$\langle (1-T)^1 \rangle = \langle (1-T)^1 \rangle_{PT} + \frac{\lambda_1}{Q} \tag{21}$$

Analogously for the second moments, we find [6]:

$$\langle (1-T)^2 \rangle = \langle (1-T)^2 \rangle_{PT} + 2\frac{\lambda_1}{Q}\langle (1-T)^1 \rangle_{PT} + \frac{\lambda_2}{Q^2} \tag{22}$$

Thus we will have for wide jet broadening:

$$\langle B_W \rangle = \langle B_W \rangle_{PT} + \frac{\lambda_1}{Q} \tag{23}$$

$$\langle B_W^2 \rangle = \langle B_W^2 \rangle_{PT} + 2\frac{\lambda_1}{Q}\langle B_W \rangle_{PT} + \frac{\lambda_2}{Q^2} \tag{24}$$

We are following this way for other event shape observables, too.

In this model the more strongly suppressed power corrections have an independent coefficient. The coefficient λ_1 is interpreted as the first moment of the shape function, λ_2 the second moment for the one hemisphere character of variables. Therefore these are universal scales [7]. The shape function model gives predictions for several observables and contains only universal free parameters λ_1, λ_2 and $\alpha_s(M_{Z^0})$. In next section, we explain the shape function model and the obtained results.

4. PHYSICS RESULTS

According to the theory [6] the shape function model includes in the model the perturbative constant as well as the non-perturbative parameters. This model is a combination of both the NLO prediction and the power correction terms.

In our analysis we are using the AMY data in the range of 51 to 60 GeV centre of mass energies, as well as the Monte Carlo (PYTHIA) simulated data in software Origin. Origin is a proprietary computer program for interactive scientific graphing and data analysis [9]. This software is widely used for fitting both the linear and non-linear equations. Doing this, we may find some parameters such as the coupling constants in the perturbative and the non perturbative part of the QCD theory.

We use the event shape variables mentioned in section 2. We calculate both the strong coupling constant $\alpha_s(M_{Z^0})$ and the non-perturbative parameter λ. We extend our calculations up to the forth-order of power corrections. The main reason behind this is to see if the coupling constant is affected by increasing the order of the power correction and also to see if there are any major differences between the lower and the higher orders in our model.

Figure 1 shows the results obtained from the JADE and OPAL experiments for the first moments for different variables [7].

As the figures indicate, all diagrams have a falling off distribution by increasing energy. The data are also fitted well within the statistical errors. In addition, we observe that the inclusion of the power correction to the NLO prediction improves consistency with the data. The experimental systematic uncertainties are estimated by the minimum overlap assumption according to Ref. [7].

Figure 2 shows the mean value of $\langle B_W \rangle$ *versus* the centre of mass energy (Q) for both Monte Carlo and the AMY data. On these diagrams are also the results obtained from the shape function model. We observe that the shape function (solid line) follows the same trend as the results obtained from the MC data. In addition the obtained values from the AMY data are consistent with both the Monte Carlo distribution and the shape function model. On the other hand, if we compare these

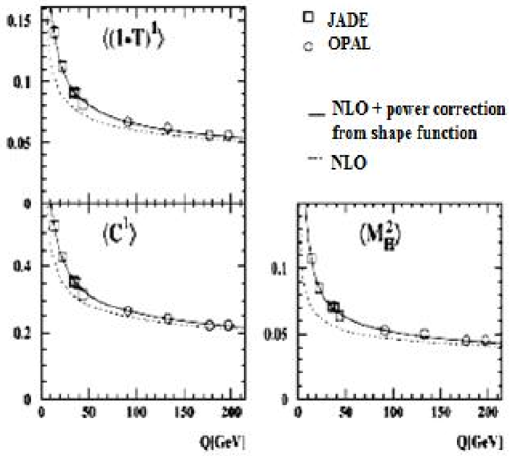

Fig. 1 – Fits of the shape function model for JADE and OPAL experiments in first moments for different variables [7].

results with NLO prediction (dash line), we conclude that the shape function model is in more agreement with the MC and the AMY data, than the NLO prediction. In this analysis, we are using the AMY data in the range of energy between 52-60 GeV obtained by a detector at the KEK storage ring, TRISTAN accelerator, Japan [10]. We are also using the simulated events (Monte Carlo: PYTHIA) which is based on the use of random numbers and probability statistics to investigate problems concerned with the hadronic interactions.

The main reason for such differences between this Model and the NLO prediction is due to the fact that the model includes in its theory, the NLO prediction, the non-perturbative part of the theory, as well as the power corrections. This makes the distributions for the model more consistent with the real data.

In addition, by increasing the order of the power correction, we observe that there is more consistency between the experiment and the theory. We conclude that the higher order corrections conform well to our real data.

By fitting the shape function model (equations: 12 and 22) with the data, we obtain the values of the strong coupling constant. Table 1 shows our results for $\langle B_W \rangle$. The errors indicated in the table are obtained from the fit to the distributions.

We observe that within statistical errors, the parameter $\alpha_s(M_{Z^0})$ is very similar, for different n values. Our results are also consistent with QCD prediction [11, 14].

Table 2 shows our results for free parameters (equation (22)) in accordance to the non-perturbative part of our analysis.

To clarify further the situation, we do a similar analysis and calculation for the $\langle B_T \rangle$, $\langle 1-T \rangle$ and $\langle \rho \rangle$. Figure 3 shows the distributions for B_T. A similar conclusion

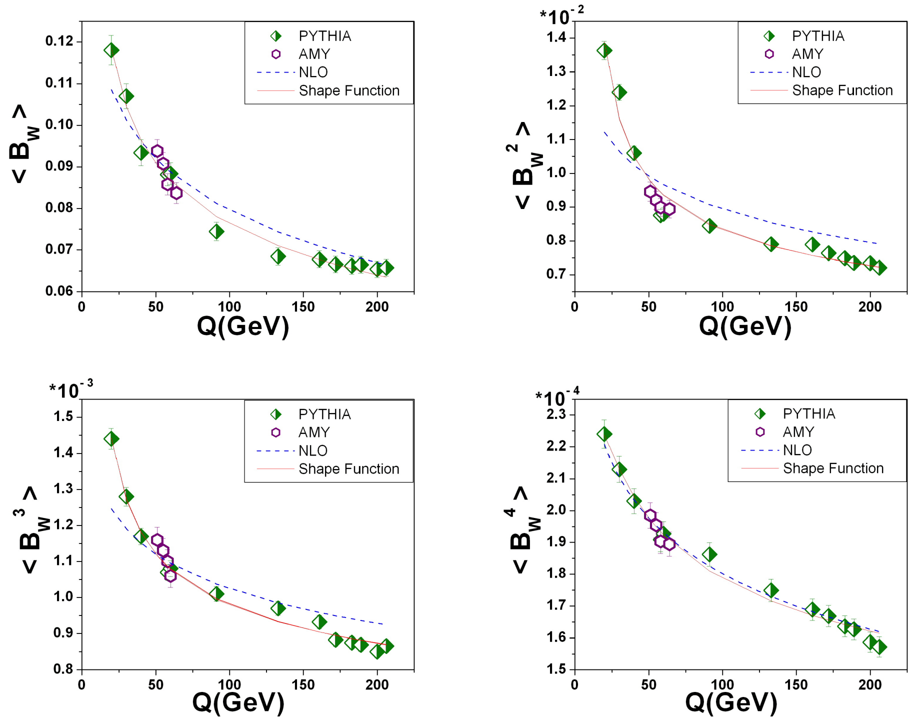

Fig. 2 – Fits of the shape function model to PYTHIA and AMY data for $\langle B_W \rangle^n$.

Table 1

$\alpha_s(M_{Z^0})$ values of variable $\langle B_W \rangle$ for different orders.

$\langle B_W \rangle^n$	$\alpha_s(M_{Z^0})$
n=1	0.12323 ± 0.00848
n=2	0.11171 ± 0.00724
n=3	0.10011 ± 0.00742
n=4	0.10004 ± 0.00812

Table 2

λ values for $(\langle B_W \rangle)^n$ moments for MC data.

Event shape variables	$\lambda_1(GeV)$	$\lambda_2(GeV)^2$
$(\langle B_W \rangle)^1$	0.48558 ± 0.01699	–
$(\langle B_W \rangle)^2$	0.45923 ± 0.01607	0.31796 ± 0.09427
$(\langle B_W \rangle)^3$	0.29664 ± 0.01038	0.15262 ± 0.01383
$(\langle B_W \rangle)^4$	0.1993 ± 0.01207	-0.28788 ± 0.0736

to the B_W variable is obtained for this variable as well as for other variable (where we exclude their distributions in this paper).

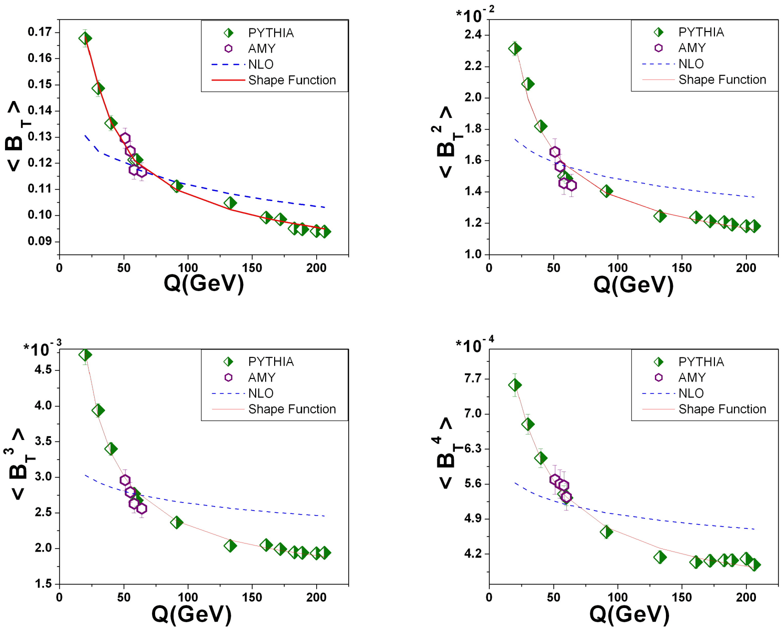

Fig. 3 – Fits of the shape function model and NLO model to MC data and AMY data for the total jet broadening.

Table 3

The values of $\alpha_s(M_{Z^0})$ up to forth orders for event shape moments.

Event shape variables	$\alpha_s(M_{Z^0})$	$\alpha_s(M_{Z^0})$	$\alpha_s(M_{Z^0})$	$\alpha_s(M_{Z^0})$
n	1	2	3	4
$\langle(1-T)^n\rangle$	0.11097 ± 0.009	0.1134 ± 0.0095	0.1323 ± 0.009	0.1346 ± 0.0085
$\langle(B_W)^n\rangle$	0.1232 ± 0.0085	0.1117 ± 0.0072	0.1001 ± 0.0074	0.10004 ± 0.0081
$\langle(\rho)^n\rangle$	0.1053 ± 0.0072	0.1062 ± 0.006	0.10824 ± 0.009	0.1115 ± 0.009
$\langle(B_T)^n\rangle$	0.1213 ± 0.006	0.1222 ± 0.006	0.1259 ± 0.006	0.1284 ± 0.009

Table 3 summarizes our overall results for the strong coupling constant up to the forth order for different event shape variables. (The parameter n on the table indicates the order of the event shape variable). Despite the fact that the distributions become more consistent by increasing n, we observe that this behavior does not have a significant effect on $\alpha_s(M_{Z^0})$. We conclude that, increasing the order of the power corrections does not affect our results considerably. The errors on the table are statistical as well as experimental. These overall values confirm well to the QCD predictions and also to the dispersive model [2].

Figure 4 shows $\alpha_s(M_{Z^0})$ in terms of n for different variables. We observe that $\langle(1-T)^n\rangle, \langle\rho^n\rangle$ and $\langle(B_T)^n\rangle$ follow a similar trend by increasing *n*. Such a behavior indicates that $\alpha_s(M_{Z^0})$ slightly increases with *n*. On the other hand $\alpha_s(M_{Z^0})$ for $\langle(B_W)^n$ shows a slight decrease with *n*. This discrepancy between the two is due to the fact that the moment for the single parameter $\langle B_W\rangle$ is not universal [7]. However such a slight decrease in $\alpha_s(M_{Z^0})$ for $\langle B_W\rangle$ is not significant to change our conclusion. The dash lines on the figures show the value of QCD prediction which is equal to $\alpha_s(M_{Z^0}) = 0.1181 \pm 0.002$ [11].

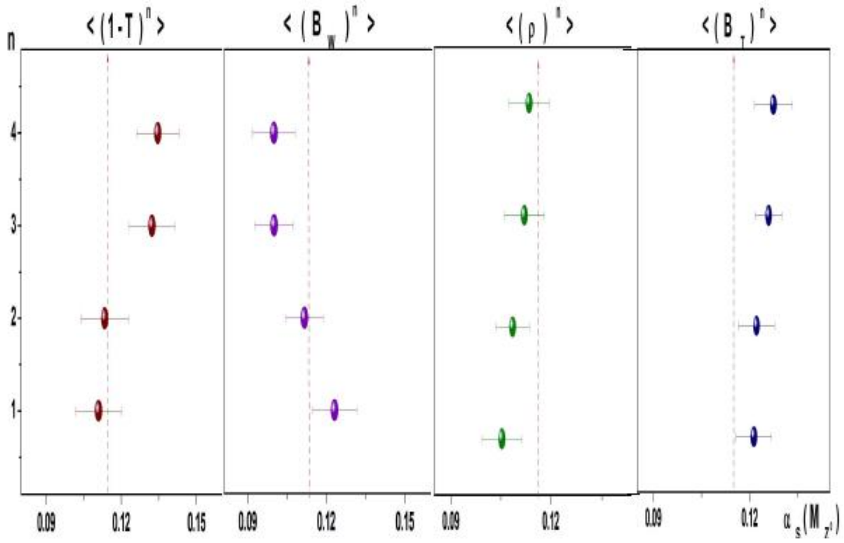

Fig. 4 – Values of $\alpha_s(M_{Z^0})$ for event shape observables up to forth order.

The above results are also consistent with those obtained from JADE and OPAL experiments for *n=1*, where the published data exists (table 4) [7].

At this stage, we are perusing on the non- perturbative part of theory. Table 5 and also figure 5 show our results for the non-perturbative parameters λ_1, defined in (22).

Table 4

The measurements of $\alpha_s(M_{Z^0})$ using shape function model with *n=1* for JADE and OPAL [7].

Event shape variables	$\alpha_s(M_{Z^0})$
$\langle 1-T\rangle$	0.1304 ± 0.0018
$\langle \rho \rangle$	0.1193 ± 0.0027

Table 5

The values of λ_1 from moments of event shape variables at MC data in different energies.

Event shape variables	**n**	$\langle (1-T)^n \rangle$	$\langle (B_W)^n \rangle$	$\langle \rho^n \rangle$	$\langle (B_T)^n \rangle$
$\lambda_1(GeV)$	1	1.4264 ± 0.0357	0.4856 ± 0.017	0.3689 ± 0.0166	1.4931 ± 0.0224
$\lambda_1(GeV)$	2	1.9681 ± 0.0236	0.4592 ± 0.0161	0.3947 ± 0.0178	1.2439 ± 0.0216
$\lambda_1(GeV)$	3	2.2675 ± 0.0272	0.2966 ± 0.0104	0.5175 ± 0.0239	1.5601 ± 0.0219
$\lambda_1(GeV)$	4	2.360 ± 0.0284	0.1993 ± 0.0121	1.0640 ± 0.0479	1.1332 ± 0.0217

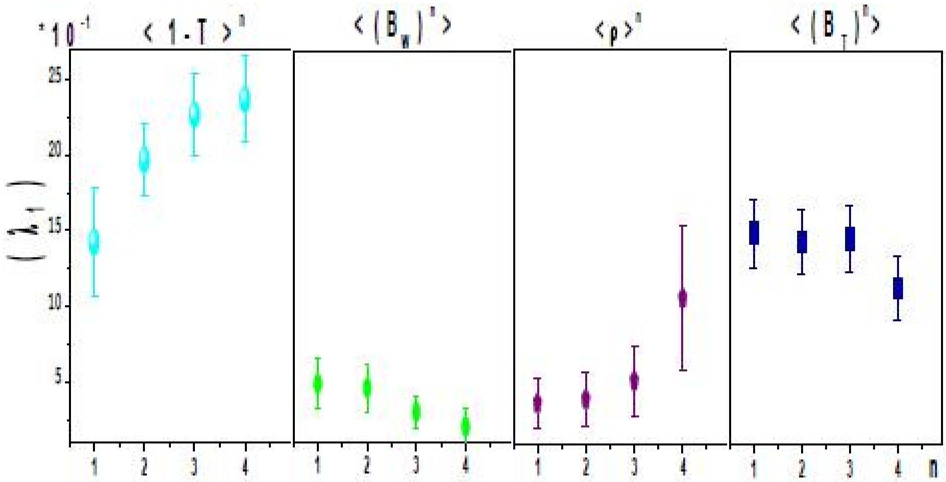

Fig. 5 – The measurements of λ_1 for four event shape observables.

Table 6 summarizes our results for the mean values of (α_s) and (λ_1), for different event shape variables.

Table 6

The mean values of α_s and λ_1 for event shape variables.

Event shape variables	$\langle(1-T)^n\rangle$	$\langle(B_W)^n\rangle$	$\langle\rho^n\rangle$	$\langle(B_T)^n\rangle$
$\alpha_s(M_{Z^0})$	0.1228 ± 0.009	0.1088 ± 0.007	0.1078 ± 0.0079	0.1245 ± 0.0069
$\lambda_1(GeV)$	2.0077 ± 0.0287	0.36019 ± 0.014	0.5863 ± 0.0265	1.3576 ± 0.0219

5. CONCLUSIONS

In this article, we have calculated both the strong coupling constant (α_s) in perturbative theory and the free parameter (λ) in non-perturbative theory, by using the shape function model. To achieve this, the event shape variables $\langle B_W\rangle$, $\langle B_T\rangle$, $\langle 1-T\rangle$ and $\langle\rho\rangle$ are employed. Next we have used the power corrections for analysis of the event shape variables up to NLO. By fitting the shape function models with the data (AMY and Monte Carlo), we extracted α_s and λ in perturbative and in non-perturbative part of the theory. We observe that the results obtained from fitting the shape function model is more accurate than the results from NLO QCD model. The reason for this is due to the fact that the former includes the non-perturbative part of the theory, as well as the NLO prediction, while the latter is just the NLO prediction. We expect that NNLO predictions give us even more accurate results. Combining the results of all variables, we have obtained the mean value of the strong coupling constant $\alpha_s(M_{Z^0}) = 0.11596\pm0.00778$, and the mean value of the non-perturbative parameter $\lambda_1 = 1.0779\pm0.02276GeV$. They are consistent with the world average value of $\alpha_s(M_{Z^0}) = 0.1181\pm0.002$ [11].

REFERENCES

1. S. Kluth, Tests of quantum chromo dynamics at e^+e colliders, *Rep. Prog. Phys*. **69** 1771-1846 (2006).
2. R. Saleh-Moghaddam and M. E. Zomorrodian, Coupling constant in dispersive model, *Pramana Journal of Physics*. **81** 5 775-790 (2013).
3. R. Saleh-Moghaddam and M. E. Zomorrodian, Thrust distribution in e^+e^- annihilation with Monte Carlo data, *Indian Journal of Physics*. **87** 7 687-690 (2013).
4. S. Kluth, P. A. Movilla Fernandez, S. Bethke, C. Pahl and P. Pfeifenschneider, A measurement of the QCD colour factors using event shape distributions at E=14 to 189 GeV, *Eur. Phys. J. C*. **21** 199-210 (2001).
5. G. Korchemsky, Shape functions and power corrections to the event shapes, *LPTHE Orsay*. **98** 44 (1998).

6. G. Korchemsky and S. Tafat, Heavy-quark and soft-collinear effective theory, *J. High Energy Phys*. **0010** 010 (2000).
7. C. Pahl, S. Bethke, O. Biebel, S. Kluth and J. Schieck, Determination of the Strong Coupling S from hadronic Event Shapes and NNLO QCD predictions using JADE Data, *Eur. Phys. J. C*. **64** 351 (2009).
8. A. Gehrmann-De Ridder, T. Gehrmann, E. W. N. Glover and G. Heinrich, NNLO moments of event shapes in e^+e^- annihilation, *JHEP*. *05* 106 (2009)
9. Origin Lab, *OriginLab Corporation One Roundhouse Plaza, Suite 303 Northampton, MA 01060 USA*, (1992).
10. K. B. Lee, H. Sagawa *et al.*, Measurement of α_S from the moment of particle momenta within jets from e^+e^- annihilation, *Physics Letters B* **313** 3 469 (1993)
11. N. Brambilla, Y. Sumino and A. Vairo, Quarkonium Spectroscopy and Perturbative QCD: A New Perspective, *Phys. Lett. B*. **513** 381-390 (2001).
12. S. Bethke, QCD tests at e+ e- colliders, *Nucl. Phys. Proc. Suppl.* **64** 54-62 (1998).
13. C. Adloff *et al.* [H1 Collaboration], Investigation of power corrections to event shape variables measured in deep inelastic scattering, *Eur. Phys. J. C*. **14** 255 (2000).
14. S. Marti i Garcia, *Review of the measurements of the strong coupling constant at LEP 2, Talks given at 5th International Workshop on Deep Inelastic Scattering and QCD (DIS97) conference (Chicago)*. hep-ex/9704016v2 (1997).